Original Article

DOI: 10.5582/bst.2021.01026

A comparative study of contrast-enhanced ultrasound and contrast-enhanced CT for the detection and characterization of renal masses

Liang Fang[1,4,§], Kun Bai[2,§], Yue Chen[1,4], Jia Zhan[1,4], Yinjia Zhang[1,4], Zhiying Qiu[1,4], Lin Chen[1,4,*], Ling Wang[3,*]

[1] Department of Ultrasound, Huadong Hospital, Fudan University, Shanghai, China;
[2] Department of Ultrasound, Jiading Central Hospital, Fudan University, Shanghai, China;
[3] Department of Reproductive Immunology, Obstetrics and Gynecology Hospital, Fudan University, Shanghai, China;
[4] Shanghai Key Laboratory of Clinical Geriatric Medicine Shanghai, China.

SUMMARY This study aims to compare the value of contrast-enhanced ultrasound (CEUS) and contrast-enhanced CT (CECT) in the differential diagnosis of benign and malignant renal masses. Included in this retrospective study were 143 renal masses in 141 patients using histopathological findings as the gold standard. A comparison was made of the two modalities in image characteristics for their accuracy in the differential diagnosis of renal masses. CEUS and CECT were both used for 39 masses in 37 patients, with 31 (79.5%) being malignant and 8 (20.5%) benign. The differences between the benign and malignant groups in perfusion intensity, perfusion uniformity and entry and exit of the contrast agent were not statistically significant ($P > 0.05$). However, CEUS could better display the circular perfusion of renal cell carcinoma than CECT ($P < 0.05$). CECT alone detected 109 masses in 107 patients, with 93 (85.3%) being malignant and 16 (14.7%) benign. CEUS detected 73 masses in 71 patients, with 56 (76.7%) being malignant and 17 (23.3%) benign. No statistically significant differences were observed between CEUS and CECT in the diagnosis of renal cell carcinoma (92.8% *vs.* 90.3%), with a specificity of 52.9% *vs.* 31.2%, an accuracy of 83.5% *vs.* 81.6%, and a positive predictive value of 86.7% *vs.* 88.4% or a negative predictive value of 69.2% *vs.* 35.7% ($P > 0.05$ for all). These results suggested both CEUS and CECT are highly valuable in the differential diagnosis of renal masses, and CEUS can be used as an important supplement for CECT in diagnosis of renal cancer.

Keywords Contrast enhanced ultrasound, renal cell carcinoma, contrast enhanced CT

1. Introduction

Renal cell carcinoma (RCC), originating from epithelial cells of proximal convolutional tubules, is a common malignant tumor of the urinary system (*1*). Clinical statistics showed that about 1/3 of patients newly diagnosed with RCC had metastases and that some may have extensive metastases without any clinical symptoms. In addition, 20-40% of patients with localized RCC develop metastasis (*2*). Therefore, enhancing diagnosis and early detection rate of RCC is key to its treatment, contributing significantly to the improved survival rate of those patients.

CT, with a high definition and spatial resolution, is able to distinguish components of the lesions such as water, fat or calcification by quantifying density of the lesions and thus able to identify the nature of the lesions (*3*). However, it is often difficult to determine the nature of RCC with a plain CT scan, and contrast-enhanced CT (CECT) with iodine contrast agent can perform better for differential diagnosis. However, as CECT is timed, it is unable to obtain a continuous scan, probably resulting in missed lesion enhancement. In addition, CECT is contraindicated for patients with an allergy to iodine contrast agent, renal insufficiency, and severe hyperthyroidism. Moreover, CECT is expensive and radioactive (*4*). Therefore, it is particularly important to seek a complementary diagnostic imaging method for CECT.

At present, conventional ultrasound (US) has become one of the commonly used imaging modalities for clinical detection and diagnosis of RCC because of its intuitiveness, simplicity, non-invasiveness, accuracy and low cost. Conventional gray-scale ultrasound remains the indispensable first choice, but its sensitivity for diagnosis of RCC is reportedly low (*5*). Color Doppler

flow imaging (CDFI) can characterize blood flow of RCC, enhancing the diagnostic accuracy of RCC to some extent. However, for small RCC located in the lower pole or ventral of the kidney, CDFI has limited diagnostic value because of difficulty in detecting the signal of internal blood flow due to thin donor vessel, deep location or low blood flow velocity (*6,7*).

Contrast-enhanced ultrasound (CEUS), a technically simple imaging modality, allows real-time acquisition without the drawbacks of CECT. CEUS with microbubble contrast agents and contrast-specific US modes have been introduced to overcome the limitations of B-mode and color Doppler US. At present, CEUS has a confirmed value in detection and diagnosis of liver cancer, and its accuracy is not inferior to that of CECT (*8,9*). The diagnostic value of CEUS in RCC is, therefore, worth exploration. The objective of this study was to investigate, by comparing with pathological findings, the sensitivity and specificity of CEUS and CECT in RCC.

2. Materials and Methods

2.1. Patients

A retrospective analysis was made of the imaging data of 141 inpatients (143 masses, 2 patients with 2 masses; all masses being ipsilateral) admitted to the Department of Ultrasound from June 2015 to June 2020. CECT and CEUS were both used for 37 patients (23 male and 14 female; aged 39-81 with an average of 62.1 ± 10.2 years) and detected 39 masses with a maximum diameter of 8-100 mm and an average of 31.0 ± 19.9 mm. CECT alone examined 107 patients (71 male and 36 female; aged 28-82 with an average of 60.0 ± 11.6 years) and detected 109 masses with a maximum diameter of 7-136 mm and an average of 43.5.6 ± 27.4 mm. CEUS alone examined 71 patients (45 male and 26 female; aged 22-83 with an average of 58.2 ± 13.1 years) and detected 73 masses with a maximum diameter of 8-100 mm and an average of (31.6 ± 17.2) mm.

The study was conducted with the approval and supervision of the ethics committee of Fudan University, and the procedure followed was in accordance with the declaration of Helsinki. After informed consent was obtained, CEUS followed by CECT was performed, and all the patients were monitored for adverse events for four hours after the procedure. The clinical status, blood pressure, and heart rate were followed up.

2.2. Ultrasound examinations

Color Doppler ultrasound was performed using the Philips iU22 (Philips Ultrasound, Bothell, Washington, USA), ACUSON S2000 (Siemens Medical Solutions, Mountain View, CA, USA) and LOGIC E9 (GE Healthcare, Milwaukee, WI, USA) ultrasound systems, all being capable of real-time contrast-enhanced imaging. The 3.5 MHz transducer was used with a mechanical index (MI) of 0.06-0.09. The contrast agent used was SonoVue (Bracco SpA, Milan, Italy),which was formulated into a suspension of Sulphur hexafluoride microbubbles (8 μL/mL) by adding 5mL of physiological saline. A baseline ultrasound examination was performed to detect lesions, and the images were saved on a hard disk. For each lesion, we measured its size, position, border, shape, echogenicity, and blood flow. CEUS was performed with a bolus injection *via* cubital vein of the contrast agent at a dose of 1.5-2.0mL flushed with 5 mL saline. In this study, we defined cortical phases as 10-15 s after injection to 30-45 s, and medullary phases as approximately 30-45 s after injection until complete disappearance of microbubble echoes. In patients with multiple lesions, an additional bolus of SonoVue (1.5-2.0mL) was administered for each lesion at an interval of at least 15 min to allow for clearance of the previous contrast injection. No contrast agent was appreciable either in the renal parenchyma or masses before starting a new examination. All the CEUS examinations were digitally recorded.

2.3. CECT examinations

All examinations were performed on a dual-source, dual-energy CT scanner (Somatom Definition, Siemens Medical Solutions, Germany). Both abdominal unenhanced CT and CECT scans were performed. Parameters included a detector collimation of 64 × 0.6 mm^2, a pitch of 1.2, a gantry rotation time of 0.5 s, a tube voltage of 120 kVp, and an abdominal reference tube current of 210 mAs. Automated tube current modulation was used in all CT studies (CARE Dose 4D; Siemens Medical Solutions). All images were reconstructed from the CECT scan with a slice thickness of 0.75-mm and a reconstruction increment of 0.5-mm. The CECT scan was started by a continuous bolus injection of 80 ml iopromide (Ultravist; 300 mg I/mL, Bayer Schering Pharma, Berlin, Germany) followed by 40 mL of saline solution into an antecubital vein *via* an 18-gauge catheter at 5 mL/s. The enhanced CT scans were performed with a delay of 25-30 s for corticomedullary phase, 55-60 s for nephrographic phase, and 240 s for excretory phase.

2.4. Image analysis and data evaluation

All the conventional ultrasound images and CEUS video clips were reviewed independently offline by two experienced radiologists blinded to the final diagnosis and not involved in the scanning. They had respectively 10 and 14 years of experience in conventional liver US and more than 7 years of experience in liver CEUS interpretation. Imaging characteristics included mass position, size, echogenicity and homogeneity, presence of

a hypoechoic rim, and color flow signals on conventional and Color Doppler ultrasound imaging. The wash-in and wash-out pattern, degree of peak enhancement, homogeneity of enhancement, and peripheral rim enhancement were evaluated by CEUS imaging. The degree of enhancement was categorized as hypo-, iso-, and hyperenhancement against that in the adjacent normal renal cortex when contrast agent reached the peak in the mass. The homogeneous enhancement was defined as complete enhancement in a lesion without any defects, and heterogeneous enhancement as a lesion with unenhanced areas, regardless of various enhancement degrees. The normal renal cortex adjacent to the tumor was used as the control for comparison of enhancement. The wash-in and wash-out pattern was classified as fast, simultaneous, or slow. The peripheral rim enhancement was considered to represent the presence of a pseudocapsule, which is determined as positive with a zone of hypoechoic ring enhancement around the lesion on CEUS and negative without.

The other two experienced radiologists in CECT studies of the liver, who were blinded to the final diagnosis, recorded and analyzed changes in the dynamic enhancement images at different phases and made independent diagnoses and conclusions. The imaging parameters included mass position, size, margins, cystic components or necrosis, calcification and attenuation on unenhanced CT scan, degree of enhancement (in Hounsfield units, HU) in different phases of the CECT scan, homogeneous or heterogeneous appearance, perinephric stranding, presence or absence of a clear capsule sign, and vascular invasion.

In case of inconsistent conclusions, a mutually accepted final conclusion was made *via* consultation. Examiners engaged in CEUS and contrast enhanced magnetic resonance imaging (CEMRI) were blind to each other's diagnosis. Diagnostic criteria for RCC: CEUS was characterized by hypoenhancement, heterogeneous enhancement, fast-in or fast-out, and peripheral ring enhancement. CECT was characterized by hypoenhancement, heterogeneous enhancement, fast-in and fast-out, and peripheral ring enhancement. All images were evaluated independently by two physicians who agreed to reach a consensus in case of a disparity.

2.5. Statistical analysis

SPSS19.0 was used, continuous data were represented by frequency, and histopathological findings were used as the standards. χ^2 test was used to compare CEUS and CECT in perfusion characteristics of benign and malignant renal masses, and their sensitivity, specificity, accuracy, positive predictive value and negative predictive value in the diagnosis of RCC. The test level was 0.05, and $P < 0.05$ was considered statistically significant.

3. Results

3.1. Histopathological findings

In 141 patients, 143 renal masses were surgically treated, and histopathology was conducted. Historically, 93 (85.3%) were malignant and 16 (14.7%) benign among the 109 masses examined by CECT alone; 56 (76.7%) malignant (Figure 1) and 17 (23.3%) benign (Figure 2) among the 73 masses examined by CEUS alone; and 31 (79.5%) malignant and 8 (20.5%) benign among 39 masses in 37 patients examined by both modalities (Table 1).

3.2. Comparison between CECT and CEUS in image characteristics of benign and malignant renal masses

Among 39 masses in 37 patients examined by both CEUS and CECT (Table 2), the 31 malignant masses featured mainly fast wash-in, fast wash-out and highly heterogeneous enhancement, and the 8 benign masses featured mainly slow or equal wash-in, slow or equal wash-out and homogeneous enhancement. However, CEUS showed better peripheral rim enhancement in the malignant renal masses than CECT ($P < 0.05$).

3.3. Comparison between CECT and CEUS in the diagnosis of RCC

CECT identified 95 malignant and 14 benign masses. Of the former, 84 were accurate diagnoses and 11 misdiagnoses including 8 angiomyolipomas (AMLs), 2 complex cysts and 1 eosinoma; of the latter, 5 were accurate diagnoses and 9 misdiagnoses, including 5 clear cell carcinomas (Figure 3F-H), 2 papillary carcinomas, 1 cystic renal carcinoma and 1 renal carcinoma of another type. CEUS identified 60 malignant and 13 benign masses. Of the former, 52 were accurate diagnoses and 8 misdiagnoses including 6 AMLs, 1 complex cyst and 1 eosinoma; of the latter, 9 were accurate diagnoses and 4 misdiagnoses including 3 clear cell carcinomas (Figure 3A-E, Figure 4A-E) and 1 collecting duct carcinoma. CEUS and CECT showed no statistically significant differences in sensitivity, specificity, accuracy, positive predictive value and negative predictive value in the diagnosis of renal malignancy ($P > 0.05$) (Table 3).

4. Discussion

Most renal tumors are malignant. Of primary renal malignant tumors, RCC accounts for 85%, renal pelvis carcinoma for 7-8%, nephroblastoma for 5-6%, and sarcoma for 3%. Among them, RCC is the most fatal urogenital malignancy, accounting for 3% of all adult tumors and 90-95% of renal cancers (*10*). The three most common subtypes of RCC are clear cell carcinoma, papillary carcinoma and chromophobe cell

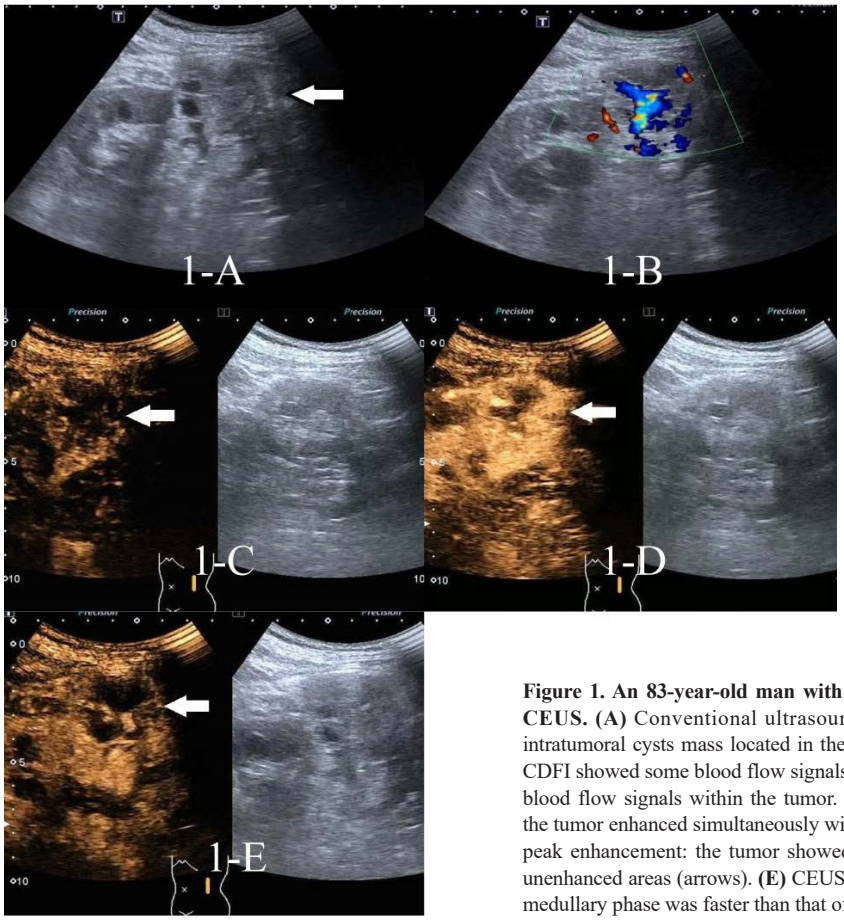

Figure 1. An 83-year-old man with a 2.6 × 1.6-cm ccRCC was diagnosed using CEUS. (A) Conventional ultrasound demonstrated a heterogeneous mass with intratumoral cysts mass located in the interpolar pole of the left kidney (arrows). **(B)** CDFI showed some blood flow signals around the tumor periphery and a few strip-like blood flow signals within the tumor. **(C)** CEUS imaging in the initial enhancement: the tumor enhanced simultaneously with the cortex (arrows). **(D)** CEUS imaging at the peak enhancement: the tumor showed heterogeneous hyperenhancement with many unenhanced areas (arrows). **(E)** CEUS imaging showed that the tumor wash-out in the medullary phase was faster than that of the renal cortex (arrows).

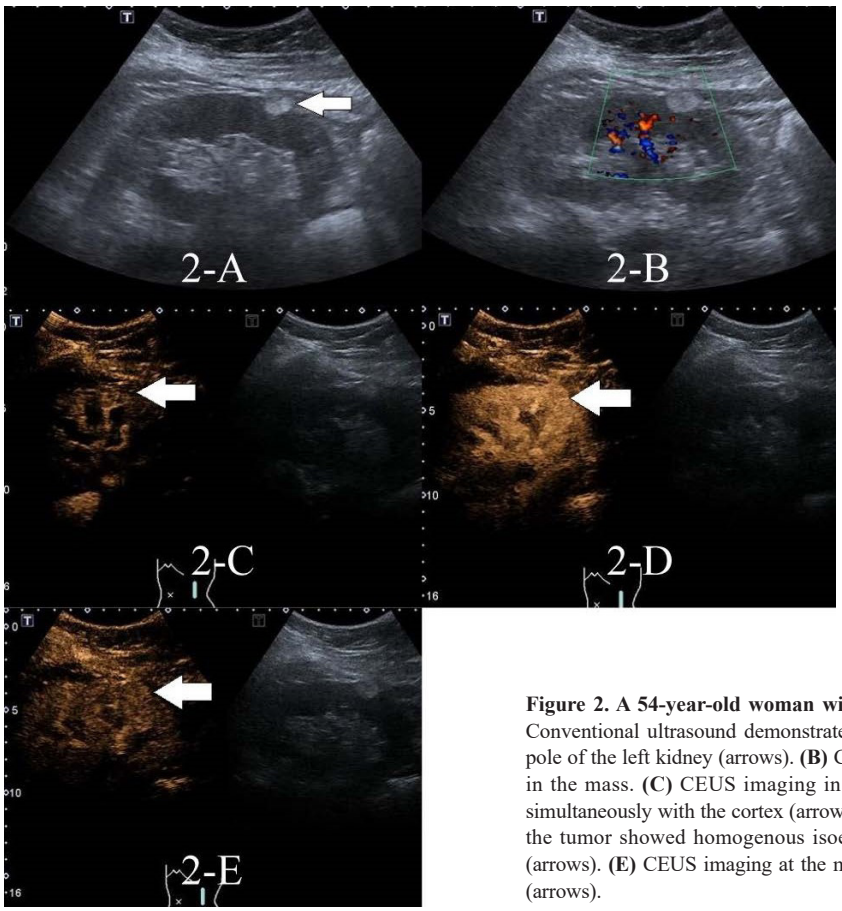

Figure 2. A 54-year-old woman with an AML was diagnosed using CEUS. (A) Conventional ultrasound demonstrated a hyperechoic mass located in the interpolar pole of the left kidney (arrows). **(B)** CDFI showed a lack of intratumoral vessel signal in the mass. **(C)** CEUS imaging in the initial enhancement: the tumor enhanced simultaneously with the cortex (arrows). **(D)** CEUS imaging at the peak enhancement: the tumor showed homogenous isoenhancement similar to the peritumoral cortex (arrows). **(E)** CEUS imaging at the medullary phase showed prolonged enhancement (arrows).

Table 1. Histopathological findings of 143 renal masses

Histopathological type		CECT	CEUS	BOTH
Malignant	ccRCC	66 (60.5)	42 (60.5)	24 (61.5)
(*n* = 31)	pRCC	7 (6.4)	5 (6.8)	3 (7.7)
	chRCC	16 (14.7)	5 (6.8)	4 (10.3)
	Collecting duct carcinoma	2 (1.8)	1 (1.4)	1 (3.6)
	Cystic RCC	1 (0.9)	1 (1.4)	0 (0)
	Other types of RCC	1 (0.9)	2 (2.7)	1 (3.6)
	ALL	93 (85.3)	56 (76.7)	31 (79.5)
Benign	AML	9 (8.3)	12 (16.4)	6 (15.4)
(*n* = 8)	Complicated cysts	6 (5.5)	4 (5.5)	1 (3.6)
	Renal oncocytoma	1 (0.6)	1 (1.4)	1 (3.6)
	ALL	16 (14.7)	17 (12.9)	8 (20.5)
	TOATL	109 (100)	73 (100)	39 (100)

AML, angiomyolipoma; ccRCC, clear cell renal cell carcinoma; pRCC, papillary renal cell carcinoma; chRCC, chromophobe renal cell carcinoma.

Table 2. Comparison between CEUS and CECT in image characteristics of benign and malignant renal masses [*N* (%)]

Histopathological results	Imaging index	Imaging features	CEUS	CECT	χ^2	*P*
Malignant	the degree of peak enhancement	hyper- enhancement	21 (67.7)	18 (58.1)	0.622	0.430
(*n* = 31)		iso-/hypo- enhancement	10 (32.3)	13 (41.9)		
	the homogeneity of enhancement	homogeneous	13 (41.9)	9 (29.0)	1.127	0.288
		inhomogeneous	18 (58.1)	22 (71.0)		
	wash-in	fast	22 (71.0)	26 (83.9)	1.476	0.224
		slow (iso-)	9 (29.0)	5 (16.1)		
	wash-out	fast	19 (61.3)	20 (64.5)	0.069	0.792
		slow (iso-)	12 (38.7)	11 (35.5)		
	Peripheral rim enhancement	Yes	12 (38.7)	5 (16.1)	3.971	0.046
		No	19 (61.3)	26 (83.9)		
Benign	degree of peak enhancement	hyper enhancement	3 (37.5)	4 (50.0)	0.254	0.614
(*n* = 8)		hypo enhancement	5 (62.5)	4 (50.0)		
	Homogeneity of enhancement	homogeneous	3 (37.5)	4 (50.0)	0.254	0.614
	wsh-in	inhomogeneous	5 (62.5)	4 (50.0)		
		fast	1 (87.5)	0 (100.0)	1.067	0.302
		slow (iso-)	7 (12.5)	8 (0)		
	wash-out	fast	1 (12.5)	2 (25.0)	0.410	0.522
		slow (iso-)	7 (87.5)	6 (75.0)		
	Peripheral rim enhancement	Yes	1 (12.5)	0 (25.0)	1.067	0.302
		No	7 (87.5)	8 (100)		

carcinoma, accounting for 70-80%, 10-15% and 5% respectively (*11*). In recent years, the rising incidence of renal malignancies has made early diagnosis and treatment increasingly important. CEUS and CECT are the main modalities for the diagnosis of renal tumors at present. CECT scanning is often used clinically to detect renal lesions, providing important evidence for the qualitative diagnosis of renal tumors. The development degree of space-occupying lesions can be inferred based on enhancement in the lesions, the presence of tumor thrombi in the renal vein and infiltration around the lesions (*12*). CEUS compensates for the low accuracy of traditional gray-scale ultrasound and color Doppler ultrasound through contrast imaging and can clearly reflect hemodynamic changes in the lesions, which is of great help to determine benign and malignant tumors (*13*). In this study, RCC was the main malignancy diagnosed by CECT and CEUS (89/93 or 95.7% *vs.* 52/56 or 92.9%), followed by papillary carcinoma, chromophobe cell carcinoma, collecting duct carcinoma, and cystic renal carcinoma. The proportions were much higher than those in SUN D' possibly because fewer cases were included in our present study. AML is the most common benign tumor of the kidney, containing different proportions of thick-walled blood vessels, smooth muscle and adipose tissue (*14*). In our study, AML was the dominant benign tumor (9/16 or 56.3% *vs.* 12/17 or 70.6%), while complex cysts and eosinophils were fewer.

At present, CEUS has been used for the differential diagnosis of benign and malignant renal lesions, and it is generally believed that CEUS is helpful in the

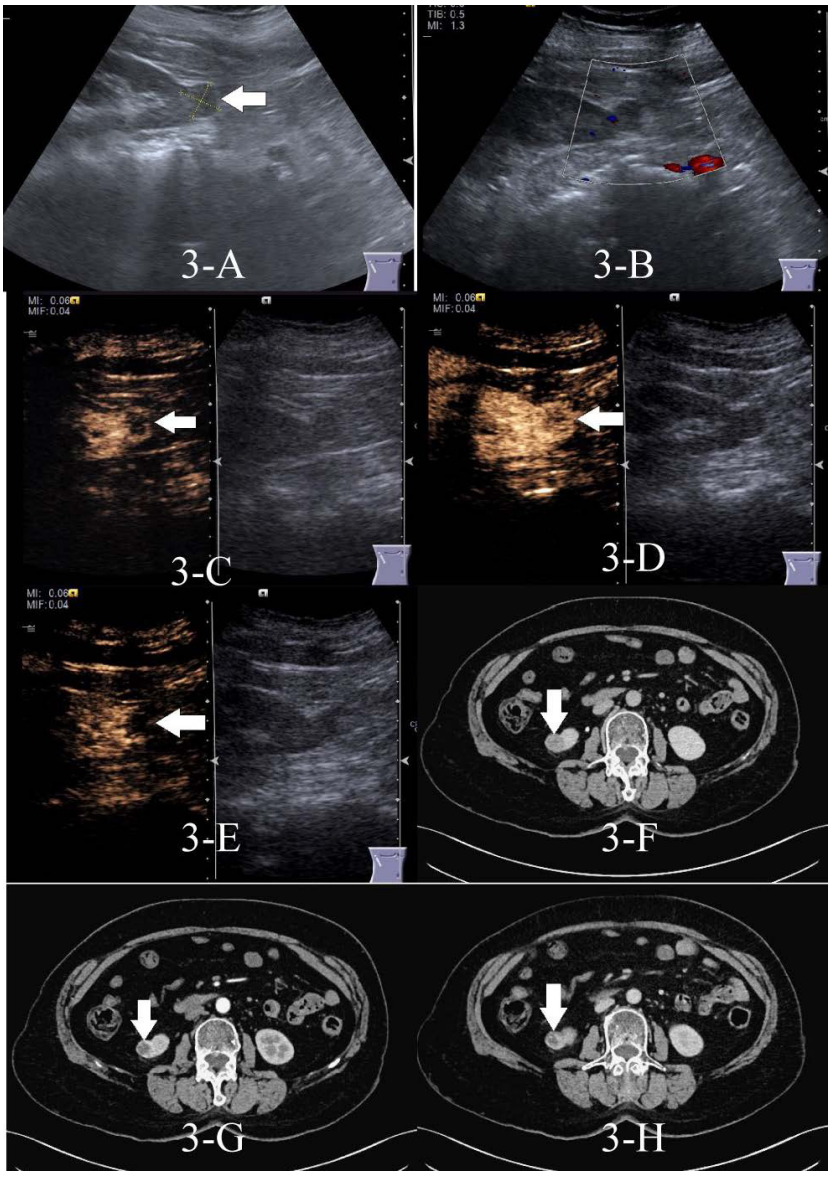

Figure 3. A 75-year-old woman with a 2.2 × 1.9-cm oncocytoma but was misdiagnosed using CEUS and CECT as RCC. (A) Conventional ultrasound demonstrated a mildly hyperechoic mass located in the lower pole of the right kidney (arrows). (B) CDFI showed a few periphery tumoral vessel signals in the mass (arrows). (C) CEUS imaging in the initial enhancement: the tumor enhanced simultaneously with the cortex (arrows). (D) CEUS imaging at the peak enhancement: the tumor showed heterogeneous hyperenhancement (arrows). (E) CEUS imaging at the medullary phase: the central region of tumor showed faster wash-out than the renal cortex (arrows). (F) Unenhanced CT demonstrated a heterogeneous mass (big arrow). (G) Corticomedullary phase: the edge of the lesion was obviously enhanced (big arrow). (H) Nephrographic phase: the tumor showed faster wash out than the renal cortex (big arrow).

diagnosis and differentiation of RCC. In this current study, among 39 masses in 37 patients detected by CEUS and CECT, the 31 malignant masses mainly featured fast wash-in, fast wash-out and heterogeneous enhancement, and the 8 benign masses mainly featured slow or equal wash-in, slow wash-out and homogeneity enhancement. Benign and malignant renal tumors have characteristic manifestations on CEUS, which was consistent with the studies by Bertolotto *et al.*, Kahna *et al.*, and Kazmierski *et al.* (*15-17*). However, some researchers believed that RCCs did not have a typical CEUS pattern and overlapped to some extent with the appearance of other renal masses (*18-21*). Haendl *et al.* (*19*) used SonoVue, a microbubble contrast agent, in 30 patients with solid renal tumors before surgery. They claimed that RCCs showed chaotic vascularization on CEUS without a typical vascularization pattern. However, only 25 RCCs, 2 uROTHelial carcinomas and 3 eosinomas were included in their study, and the results might not be universal. Quaia *et al.* (*20*) performed Levovist-enhanced pulse-inverted harmonic imaging on 26 patients with renal masses, and they reported that CEUS was still limited in differentiating between solid and cystic renal masses. Therefore, further study of a larger sample size and the inclusion of other types of renal lesions are necessary to validate the results of this series.

Heterogeneous perfusion was associated with the presence of hemorrhage, necrosis, and cystic changes in the mass (*22*). In this study, inhomogeneous perfusion in the benign and malignant renal masses was not statistically significant. The reason lies in the rapid growth of malignant tumors and their increasing demand for nutrients. When the needs cannot be met, changes such as necrosis and cystic degeneration will occur inside the tumor (*21,23,24*). Internal echoes in most AMLs were uniform, but some AMLs, especially those larger than 4cm, may also have spontaneous hemorrhage, and CEUS presents inhomogeneous perfusion (*25*).

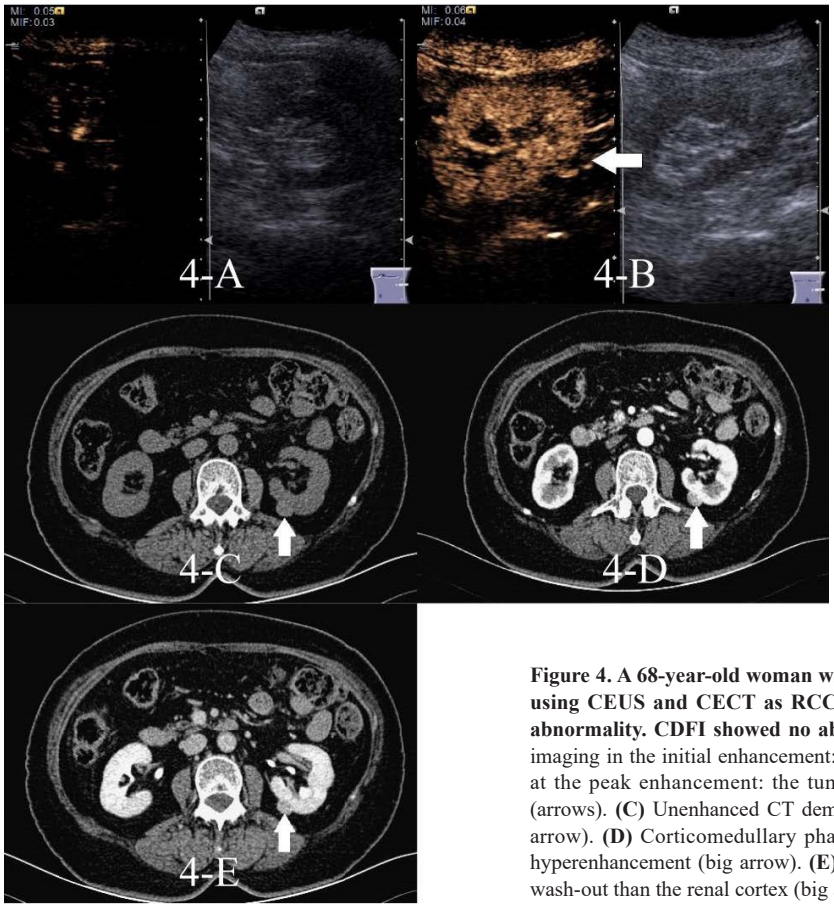

Figure 4. A 68-year-old woman with a 1.7 × 1.3-cm AML but was misdiagnosed using CEUS and CECT as RCC. Conventional ultrasound demonstrated no abnormality. CDFI showed no abnormal vessel signals in the mass. (A) CEUS imaging in the initial enhancement: the cortex enhanced in 19s. **(B)** CEUS imaging at the peak enhancement: the tumor showed heterogeneous hyperenhancement (arrows). **(C)** Unenhanced CT demonstrated a homogenous low density mass (big arrow). **(D)** Corticomedullary phase: the mass showed obviously heterogeneous hyperenhancement (big arrow). **(E)** Nephrographic phase: the tumor showed faster wash-out than the renal cortex (big arrow).

Table 3. Comparison of the accuracy between CEUS and CECT in the diagnosis of RCC

Methods	Sensitivity	specificity	accuracy	PPV	NPV
CECT	84/93(90.3%)	5/16(31.2%)	89/109(81.6%)	84/95(88.4%)	5/14(35.7%)
CEUS	52/56(92.8%)	9/17(52.9%)	61/73(83.5%)	52/60(86.7%)	9/13(69.2%)
χ^2	0.282	1.588	0.110	0.105	3.033
P	0.595	0.208	0.740	0.746	0.128

Peripheral rim enhancement, referring to the annular enhanced area around the tumor, is pathologically based on the high degree of malignancy and rapid growth of RCC masses, which compresses the adjacent normal renal tissue and leads to ischemia, necrosis and fibrosis, and the formation of a false envelope (*26,27*). Circumferential perfusion can better indicate renal malignancy. It may also be a standard for kidney preservation surgery (*28*). In our study, CEUS could display annular perfusion better than CECT ($P < 0.05$). Tamai *et al.* (*29*) used a high-MI CEUS technique and Levovist (SHU 508A; Schering AG, Berlin, Germany) and found tumor blood flow in all 29 patients with renal lesions, while contrast CT failed to show it in 5 patients, and among clear cell carcinomas, hypervascularity on CEUS was observed in 17 of 18 patients. Consistent with our study, CEUS was believed to be able to detect blood flow with contrast microbubbles, the true blood pool agent and could show more characteristic features of RCCs than CECT.

In this study, pathological findings were used as the gold standard to determine the sensitivity (92.8% *vs.* 90.3%), specificity (52.9% *vs.* 31.2%), accuracy (83.5% *vs.* 81.6%), positive predictive value (86.7% *vs.* 88.4%), and negative predictive value (69.2% *vs.* 35.7%) of CEUS and CECT in the diagnosis of RCC, with no statistical difference between the five groups. Therefore, CEUS is expected to be an independent imaging modality for the diagnosis of RCC. However, when RCC is associated with hemorrhage, liquefaction and necrosis, it loses its typical characteristics and, on CEUS, often shows atypical enhancement patterns.

In this study, most RCCs showed fast wash-in and fast wash-out and hyperenhancement, and almost all of the cases were diagnosed as clear cell carcinoma with a high diagnostic accuracy. The misdiagnoses were basically those with hypoenhancement, that is, those with fewer blood vessels. In the CEUS group, 6

AMLs were misdiagnosed as RCCs, and 3 RCCs as AML. In the CECT group, 8 AMLs were misdiagnosed as RCC, and 4 RCCs as AML. It is worth noting that AMLs were misdiagnosed as RCC when both CEUS and CECT were used. It is of great significance to distinguish AMLs from RCCs. AMLs, composed of malformed blood vessels, spindle smooth muscle and fat cells, can be simply divided into "typical AMLs" and "atypical AMLs" (*30*). As most AMLs, referred to as "typical AML," contain a large amount of adipose tissue, they can be detected by CT or MRI (*31*). However, studies have also shown that about 5% of AMLs are fat-free and are often misdiagnosed as RCC (*32*). In this study, 2 AMLs with fast wash-in, fast wash-out and hyperenhancement on CEUS and CECT were misdiagnosed as RCC, and it was speculated that the AMLs were rich in blood vessels. Lee-Felker SA *et al.* suggested that accurate measurements of CT values on plain and enhanced scans of the cortex-medulla, parenchyma, and excretory phases may help to distinguish clear cell renal cell carcinoma (ccRCC), papillary renal cell carcinoma (pRCC), chromophobe renal cell carcinoma (chRCC), renal oncocytoma, and minimal fat AMLs (*33*). However, due to the small sample size of their study and the fact that the speed of renal contrast media wash-in and wash-out of the kidneys may be influenced by the patient's own factors, more research is needed to determine whether quantitative analysis CT can be used to differentiate AML from RCC. Xu ZF *et al.* believed that AMLs have no false envelop in pathology, and the false envelop can be used to accurately identify RCC and AML (*21*), but some RCCs have no false envelop, which makes it difficult to accurately identify RCC and AML on CEUS and CECT.

Totally 3 complicated cysts were misdiagnosed as RCC, 1 being in the CEUS group and 2 in the CECT group. Complicated cysts, according to their progression possibility, fall into levelI, II, III, and IV, with a progression probability of 0%, 15%, 50% and 95%, respectively. RCC is the most common sequel of progression, this could be the reason that complicated cysts and RCCs are difficult to distinguish on both CEUS and CECT, especially with high-level (IIIand above) complicated cysts. Multilocular cystic renal cell carcinoma (MCRCC), a special type of RCCs, is almost entirely cystic with varying lumen sizes and fluid filling. Nodules of soft tissues can be seen in the cyst wall and uneven thickening of the septum. A few cystic walls or septal calcifications are seen. The boundary is generally clear, being separated with fibrous capsule from surrounding normal renal tissues, and irregular enhancement of cyst wall and septum can be observed. Complicated cysts, especially those of level IIIand above, have similar presentations to multilocular RCC and are difficult to distinguish on CEUS and CECT. This may account for the misdiagnoses in this study.

Three limitations are mentionable. First, only the masses histopathologically confirmed after surgical resection were enrolled in this study, which might have resulted in selection bias. Many benign lesions at follow-up without histopathologic diagnosis were excluded; thus, the sample of AMLs was relatively smaller than that of RCCs. Second, this study included few cases examined by both CEUS and CECT, and a larger sample size is needed for further investigation. Finally, our study was retrospective in nature.

In conclusion, CEUS and CECT play an equally important role in the diagnosis of RCCs. CEUS may serve as a substitute for CECT when the latter is impossible in iodipin-allergic patients or in patients with renal inadequacy. A small number of atypical RCCs require employment of the two imaging modalities as justified by the patient's medical history, clinical manifestations and findings in laboratory tests. Such comprehensive judgment by the radiologist, sonographer, and clinician improves the diagnosis of RCC.

Funding: This work was supported by the 2016 program of the Shanghai Municipal Health and Family Planning Commission (grant no.201640285 to Lin Chen).

Conflict of Interest: The authors have no conflicts of interest to disclose.

References

1. Motzer RJ, Jonasch E, Agarwal N, *et al.* Kidney cancer, version 3.2015. J Natl Compr Canc Netw. 2015; 13:151-159.
2. Wasserman M, Sobel D, Pareek G. Choice of Surgical Options in Kidney Cancer and Surgical Complications. Semin Nephrol. 2020; 40:42-48.
3. Leveridge MJ, Bostrom PJ, Koulouris G, Finelli A, Lawrentschuk N. Imaging renal cell carcinoma with ultrasonography, CT and MRI. Nat Rev Urol. 2010; 7:311-325.
4. Marschner CA, Ruebenthaler J, Schwarze V, Negrão de Figueiredo G, Zhang L, Clevert DA. Comparison of computed tomography (CT), magnetic resonance imaging (MRI) and contrast-enhanced ultrasound (CEUS) in the evaluation of unclear renal lesions. Rofo. 2020; 192:1053-1059.
5. Chen L, Wang L, Diao X, Qian W, Fang L, Pang Y, Zhan J, Chen Y. The diagnostic value of contrast-enhanced ultrasound in differentiating small renal carcinoma and angiomyolipoma. Biosci Trends. 2015 9:252-258.
6. Sparchez Z, Radu P, Sparchez M, Crisan N, Kacso G, Petrut B. Contrast enhanced ultrasound of renal masses. A reappraisal of EFSUMB recommendations and possible emerging applications. Med Ultrason. 2015; 17:219-226.
7. Lu Q, Wang WP, Huang BJ, Li CL, Li C. Minimal fat renal angiomyolipoma: the initial study with contrast-enhanced ultrasonography. Ultrasound Med Biol. 2012; 38:1896-1901.
8. Wilson SR, Burns PN, Kono Y. Contrast-Enhanced Ultrasound of Focal Liver Masses: A Success Story. Ultrasound Med Biol. 2020; 46:1059-1070.

9. Yang DP, Zhuang BW, Wang W, Xie XY, Xie XH. Differential diagnosis of liver metastases of gastrointestinal stromal tumors from colorectal cancer based on combined tumor biomarker with features of conventional ultrasound and contrast-enhanced ultrasound. Abdom Radiol (NY). 2020; 45:2717-2725.
10. Vázquez Estévez S, Anido U, Lázaro M, Fernández O, Fernández Núñez N, de Dios Álvarez N, Varela V, Campos Balea B, Agraso S, Areses MC, Iglesias L, Blanco M, Maciá S, Anton Aparicio LM. A new scenario in metastatic renal cell carcinoma: a SOG-GU consensus. Clin Transl Oncol. 2020; 22:1565-1579.
11. Sun D, Wei C, Li Y, Lu QJ, Zhang W, Hu B. Contrast-enhanced Ultrasonography with Quantitative Analysis allowing Differentiation of Renal Tumor Tumor types. Sci Rep. 2016; 6:35081.
12. Jin L, Xie F. Untargeted Contrast-Enhanced Ultrasound Versus Contrast-Enhanced Computed Tomography: A Differential Diagnostic Performance (DDP) Study for Kidney Lesions. Clinics (Sao Paulo). 2020; 75:e1489.
13. Wei SP, Xu CL, Zhang Q, Zhang QR, Zhao YE, Huang PF, Xie YD, Zhou CS, Tian FL, Yang B. Contrast-enhanced ultrasound for differentiating benign from malignant solid small renal masses: comparison with contrast-enhanced CT. Abdom Radiol (NY). 2017; 42:2135-2145.
14. Boudaouara O, Kallel R, Dhieb D, Smaoui W, Ayed HB, Keskes L, Sellami Boudawara T. Renal angiomyolipoma: Clinico-pathologic study of 17 cases with emphasis on the epithelioid histology and p53 gene abnormalities. Ann Diagn Pathol. 2020; 47:151538.
15. Bertolotto M, Bucci S, Valentino M, Currò F, Sachs C, Cova MA. Contrast-enhanced Ultrasound for characterizing renal masses. Eur J Radiol. 2018; 105:41-48.
16. Kahna AE, Ostrowski, AK, Caserta MP, Galler, IJ, Thiel, DD. Contrast enhanced ultrasound characterization of surgically resected renal masses in patients on dialysis. Scand J Urol. 2019; 53:344-349.
17. Kazmierski B, Deurdlian C, Tchelepi H, Grant EG. Applications of contrast-enhanced ultrasound in the kidney. Abdom Radiol (NY). 2018; 43:880-898.
18. Cokkinos DD, Antypa EG, Skilakaki M, Kriketou D, Tavernaraki E, Piperopoulos PN. Contrast Enhanced Ultrasound of the Kidneys: What is it capable of? Biomed Res Int. 2013; 2013:595873.
19. Haendl T, Strobel D, Legal W, Frieser M, Hahn EG, Bernatik T. Renal cell cancer does not show a typical perfusion pattern in contrast-enhanced ultrasound. Ultraschall Med. 2009; 30:58-63.
20. Quaia E, Siracusano S, Bertolotto M, Monduzzi M, Mucelli PR. Characterization of renal tumours with pulse inversion harmonic imaging by intermittent high mechanical index technique: initial results. Eur Radiol. 2003; 13:1402-1412.
21. Xu ZF, Xu HX, Xie XY, Liu GJ, Zheng YL, Liang JY, Lu MD. Renal cell carcinoma: real-time contrast-enhanced ultrasound findings. Abdom Imaging. 2010c; 35:750-756.
22. Li CX, Lu Q, Huang BJ, Xue LY, Yan LX, Zheng FY, Wen JX, Wang WP. Quantitative evaluation of contrast-enhanced ultrasound for differentiation of renal cell carcinoma subtypes and angiomyolipoma. Eur J Radiol. 2016; 85:795-802.
23. Jiang J, Chen YQ, Zhou YC, Zhang HZ. Clear cell renal cell carcinoma: contrast-enhanced ultrasound features relation to tumor size. Eur J Radiol. 2010; 73:162-167.
24. Xue LY, Lu Q, Huang BJ, Li CX, Yan LX, Wang WP. Differentiation of subtypes of renal cell carcinoma with contrast-enhanced ultrasonography. Clin Hemorheol Microcirc. 2016; 63:361-371.
25. King KG, Gulati M, Malhi H, Hwang D, Gill IS, Cheng PM, Grant EG, Duddalwar VA. Quantitative assessment of solid renal masses by contrast-enhanced ultrasound with time-intensity curves: how we do it. Abdom Imaging. 2015; 40:2461-2471.
26. Yamashita Y, Honda S, Nishiharu T, Urata J, Takahashi M. Detection of pseudocapsule of renal cell carcinoma with MR imaging and CT. AJR Am J Roentgenol. 1996; 166:1151-1155.
27. Dai WB, Yu B, Diao XH, Cao H, Chen L, Chen Y, Zhan J. Renal Masses: Evaluation with Contrast-Enhanced Ultrasound, with a Special Focus on the Pseudocapsule Sign. Ultrasound Med Biol. 2019; 45:1924-1932.
28. Pretorius ES, Siegelman ES, Ramchandani P, Cangiano T, Banner MP. Renal neoplasms amenable to partial nephrectomy: MR imaging. Radiology.1999; 212:28-34.
29. Tamai H, Takiguchi Y, Oka M, *et al.* Contrast-enhanced ultrasonography in the diagnosis of solid renal tumors. J Ultrasound Med. 2005; 24:1635-1640.
30. Srigley JR, Delahunt B, Eble JN, Egevad L, Epstein JI, Grignon D, Hes O, Moch H, Montironi R, Tickoo SK, Zhou M, Argani P; ISUP Renal Tumor Panel. The International Society of Urological Pathology (ISUP) Vancouver Classification of Renal Neoplasia. Am J Surg Pathol. 2013; 37:1469-1489.
31. Lane BR, Aydin H, Danforth TL, Zhou M, Remer EM, Novick AC, Campbell SC. Clinical correlates of renal angiomyolipoma subtypes in 209 patients: classic, fat poor, tuberous sclerosis associated and epithelioid. J Urol. 2008; 180:836-843
32. Nicolau C, Pano B, Sebastia C. Managing focal incidental renal lesions. Radiologia. 2016; 58:81-87
33. Lee-Felker SA, Felker ER, Tan N, Margolis DJ, Young JR, Sayre J, Raman SS. Qualitative and quantitative MDCT features for differentiating clear cell renal cell carcinoma from other solid renal cortical masse. AJR Am J Roentgenol. 2014; 203:W516-24.

Received January 15, 2021; Revised February 18, 2021; Accepted February 24, 2021.

[§]These authors contributed equally to this work.
**Address correspondence to:*
Lin Chen, Department of Ultrasound, Huadong Hospital, Fudan University, 211 West Yan'an Rd, Shanghai 200040, China.
E-mail: cl_point@126.com

Ling Wang, Laboratory for Reproductive Immunology, Hospital & Institute of Obstetrics and Gynecology, Fudan University, 419 Fangxie Road, Shanghai 200011, China.
E-mail: Dr.wangling@fudan.edu.cn

Released online in J-STAGE as advance publication February 26, 2021.